Linear polarization of photoluminescence in quantum wires

1997 J. Phys.: Condens. Matter 9 5105

(http://iopscience.iop.org/0953-8984/9/24/010)

J. Phys.: Condens. Matter **9** (1997) 5105–5116. Printed in the UK PII: S0953-8984(97)73713-5

Linear polarization of photoluminescence in quantum wires

W H Zheng, Jian-Bai Xia† and K W Cheah‡

Department of Physics, Hong Kong Baptist University, Kowloon Tong, Hong Kong§

Received 16 April 1996, in final form 10 December 1996

Abstract. The linear character of the polarization of the luminescence in porous Si is studied experimentally, and the corresponding luminescence characteristics in quantum wires are studied theoretically using a quantum cylindrical model in the framework of the effective-mass theory. From the experimental and theoretical results it is concluded that there is a stronger linear polarization parallel to the wire direction than there is perpendicular to the wire, and that it is connected with the valence band structure in quantum confinement in two directions. The theoretical photoluminescence spectra of the parallel and perpendicular polarization directions, and the degree of polarization as functions of the radius of the wire and the temperature are obtained for $In_{0.53}Ga_{0.47}As$ quantum wires and porous silicon. From the theory, we demonstrated that the degree of polarization decreases with increasing temperature and radius, and that this effect is more apparent for porous Si. The theoretical results are in good agreement with the experimental results for the InGaAs quantum wires, and in qualitative agreement with those for the porous silicon.

1. Introduction

The investigation of low-dimensional semiconductor structures such as quantum wires has attracted much attention in recent years. The interest is raised both by their potential as regards uncovering new phenomena in condensed-matter physics, and by their potential device applications [1, 2]. The quantum wires have one-dimensional energy subbands with singular densities of states; hence it is expected that they will have higher luminescence efficiencies than general quantum wells. There have been many reports involving fabrication of such structures by methods such as electron-beam lithography [3–7], combined with impurity-induced interdiffusion [8], and overgrowth of previously etched patterns [9], or on non-(100)-oriented substrates [10], and of structures formed via strain-induced lateral confinement [11]. Canham [12] first reported the visible light emitted by porous silicon, in 1990; this is another kind of quantum wire or dot material.

The luminescence of quantum wires has a common characteristic: the linear polarization along the directions parallel and perpendicular to the wire direction are obviously different, and this can be used to distinguish the luminescence from the quantum wells or quantum wires. For the $GaAs/Al_xGa_{1-x}As$ quantum wires with lateral dimensions of 70 nm [6], the one-dimensional character was reflected in a strong polarization dependence, and the intensity of the light polarized parallel to the wires is larger than that of the light polarized perpendicular to the wires. In the quantum wires with strain-induced lateral confinement

† Permanent address: Institute of Semiconductors, Chinese Academy of Sciences, PO Box 912, 100083 Beijing, People's Republic of China.

‡ Author to whom any correspondence should be addressed.

§ Fax: +852/23046558; e-mail: kwcheah@hkbc.edu.hk.

0953-8984/97/245105+12$19.50

[11], extreme changes were observed in the transition intensities and polarization anisotropy of the strained quantum wires as compared to those for the unstrained quantum wells. The light-hole transitions are stronger than the heavy-hole ones, and the degree of polarization along the wires is more than five times that perpendicular to the wires. The $In_xGa_{1-x}As/InP$ quantum wire structures fabricated by a combination of high-resolution electron-beam lithography and deep wet etching [7] show a strong linear polarization parallel to the wires. The polarization is proportional to $1/L_x$ (L_x is the lateral width of the wire) for broad wires, and becomes saturated in the case of narrow wires. Anisotropic linear polarization of the porous Si photoluminescence (PL) has also been reported [13–15]. The degree of polarization as a function of the excitation wavelength, emission wavelength, and the polarization of the exciting light, etc, is obtained. In some cases, however, the PL is preferentially polarized along the [100] (wire) direction, regardless of the polarization of the exciting light.

In this paper we first look theoretically at the linear polarization of the PL in quantum wires using the quantum cylindrical model [16], then study experimentally the linear polarization of the PL in porous Si. Section 2 gives the theoretical model. Section 3 gives the theoretical calculations for the $In_xGa_{1-x}As$ quantum wires, and a comparison with the experimental results. Section 4 gives the experimental results for porous Si. Section 5 gives the theoretical calculations for porous silicon, and a comparison with our experiments.

2. The theoretical model [16]

The hole effective-mass Hamiltonian in the zero-spin–orbital-coupling (zero-SOC) limit is

$$H_h = \frac{\gamma_1}{2m_0}\begin{vmatrix} P_1 & S & T \\ S^* & P_3 & S \\ T^* & S^* & P_1 \end{vmatrix} \tag{1}$$

where

$$\begin{aligned} P_1 &= \left(1+\frac{\mu}{2}\right)(p_x^2+p_y^2)+(1-\mu)p_z^2 \\ P_3 &= (1-\mu)(p_x^2+p_y^2)+(1+2\mu)p_z^2 \\ S &= \frac{3}{\sqrt{2}}\mu(p_x-\mathrm{i}p_y)p_z \\ T &= \frac{3}{2}\mu(p_x-\mathrm{i}p_y)^2 \end{aligned} \tag{2}$$

and the basic functions of the valence band top are $|11\rangle$, $|10\rangle$, and $|1\,{-1}\rangle$, with components of angular momentum 1, 0, and -1, respectively. Here we have made the spherical symmetry assumption, in which $\gamma_2=\gamma_3$, and $\mu = 2\gamma_2/\gamma_1$, where γ_1, γ_2, γ_3 are the Luttinger effective-mass parameters [17].

In order to take into account the effect of finite SOC, we start from the hole Hamiltonian (1) in the zero-SOC limit, and then we add the SOC Hamiltonian:

$$H_{SO} = \begin{vmatrix} -\lambda & 0 & 0 & 0 & 0 & 0 \\ 0 & 0 & 0 & \sqrt{2}\lambda & 0 & 0 \\ 0 & 0 & \lambda & 0 & -\sqrt{2}\lambda & 0 \\ 0 & \sqrt{2}\lambda & 0 & \lambda & 0 & 0 \\ 0 & 0 & -\sqrt{2}\lambda & 0 & 0 & 0 \\ 0 & 0 & 0 & 0 & 0 & -\lambda \end{vmatrix} \tag{3}$$

the first three bases are spin-up, and the last three bases are spin-down, where

$$\lambda = \frac{\eta^3}{4m_0^2c^2}\langle X|\frac{\partial V}{\partial x}\frac{\partial}{\partial y}|Y\rangle = \frac{\Delta}{3}. \tag{4}$$

Δ is the spin–orbital splitting energy of the valence band top.

We consider a cylinder model, with radius R, and assume that the cylinder has a sharp boundary, so that the wave functions at the boundary are zero. In the cylindrical coordinate system we can expand the wave function in terms of Bessel functions. In the zero-SOC limit, the solution of the zero-SOC Hamiltonian (1) is as follows:

$$\Phi_{L,k_z} = \sum_n \begin{vmatrix} b_n A_{L-1,n} J_{L-1}(k_n^{L-1}r)\mathrm{e}^{\mathrm{i}(L-1)\theta} \\ c_n A_{L,n} J_L(k_n^L r)\mathrm{e}^{\mathrm{i}L\theta} \\ d_n A_{L+1,n} J_{L+1}(k_n^{L+1}r)\mathrm{e}^{\mathrm{i}(L+1)\theta} \end{vmatrix} \mathrm{e}^{\mathrm{i}k_z z} \tag{5}$$

where $A_{L,n}$ is the normalization constant:

$$A_{L,n} = \frac{1}{\sqrt{\pi}RJ_{L+1}(\alpha_n^L)} \tag{6}$$

where $\alpha_n^L = k_n^L R$ is the zero point of the Bessel function $J_L(r)$, and r is the radial coordinate. The wave vector along the z-direction, k_z, and the azimuthal angular momentum L are conserved quantum numbers.

In the presence of SOC, we construct the wave function

$$\Phi_{L+1/2} = a\Phi_L\uparrow + b\Phi_{L+1}\downarrow. \tag{7}$$

Inserting wave function (7) and expression (5) into the effective-mass envelope function equations, and by using

$$(p_x \pm \mathrm{i}p_y)J_L(kr)\mathrm{e}^{\mathrm{i}L\theta} = \mu\frac{\eta}{\mathrm{i}}kJ_{L\pm1}(kr)\mathrm{e}^{\mathrm{i}(L\pm1)\theta} \tag{8}$$

we easily obtain the secular equation for the coefficients b_n, c_n, and d_n in equation (5).

The wave function of the electronic state is simply

$$\Phi_{L,n} = A_{L,n}J_L(k_n^L r) \tag{9}$$

with the eigen-energy

$$E_{L,n} = \frac{(\eta k_n^L)^2}{2m_e^*} \tag{10}$$

where m_e^* is the electronic effective mass.

3. Theoretical results for InGaAs quantum wires

Ils *et al* found a strong linear polarization parallel to the $In_{0.53}Ga_{0.47}As$ quantum wires fabricated by electron-beam lithography [7]. When the lateral width approaches the quantum well thickness of 5 nm, the degree of linear polarization which is defined as

$$P = \frac{I_\parallel - I_\perp}{I_\parallel + I_\perp} \tag{11}$$

reaches a maximum value of 0.6 ($I_{||}$ and $I_\perp$ are the PL intensities parallel and perpendicular to the wire, respectively). We use our quantum cylindrical model with a sharp boundary to simulate the InGaAs quantum wire with a square cross section, and calculate the PL spectra for different widths (radii) and temperatures.

The PL spectrum as a function of energy is given by

$$\mathrm{PL}(E) = C \sum_{i,j} f_e(E_i) f_h(E_j) Q_{ij} \frac{\Gamma/\pi}{(E - E_i - E_j)^2 + \Gamma^2} \tag{12}$$

where C is a constant, E_i and E_j are the energies of electron and hole states, $f_e(E_i)$ and $f_h(E_j)$ are their distribution functions, respectively, and Q_{ij} is the optical transition matrix element. The Lorentz lineshape is used with the linewidth Γ. Since InGaAs is intrinsic, the electron and hole distribution functions can be represented by the Maxwell distribution. For the electron,

$$f_e(E_i) = \left\{ \exp\left[-\left(E_n + \frac{\eta^2 k_z^2}{2m_e^*} \right) \Big/ k_B T \right] \right\} \Big/ \left\{ \sqrt{2m_e^* k_B T/\pi\eta^2} \sum_n \exp(-E_n/k_B T) \right\}. \tag{13}$$

However, for the hole, the one-dimensional subbands are not parabolic, as will be seen below. Therefore the hole distribution function is

$$f_h(E_j) = \exp(-E_{n,k_z}/k_B T) \Big/ \sum_{n,k} \exp(-E_{n,k_z}/k_B T). \tag{14}$$

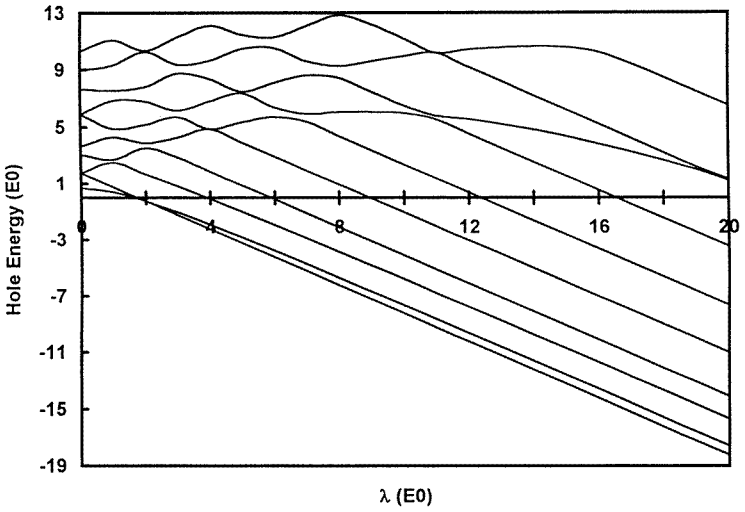

Figure 1. Hole subbands at $k_z = 0$, $L = 0$ for an $In_{0.53}Ga_{0.47}As$ quantum cylinder, as functions of the spin–orbital splitting parameter (in units of E_0).

Table 1. Effective-mass parameters used in the calculation.

	γ_1	γ_2	γ_3	μ	m_e^*	Δ (meV)
GaAs	6.85	2.10	2.90		0.067	341
InAs	19.67	8.37	9.29		0.023	380
InGaAs	13.64	5.42	6.29	0.8805	0.044	362
Si	4.22	1.02	1.02	0.4834	0.2	44

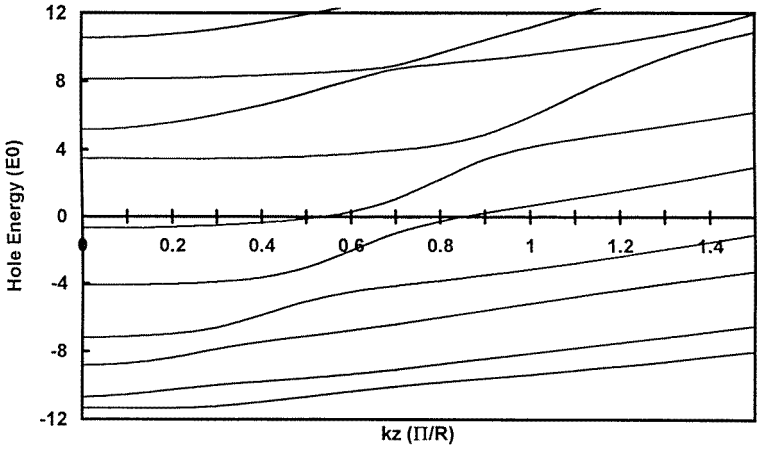

Figure 2. Hole subbands at $\lambda = 13$, $L = 0$ for an $In_{0.53}Ga_{0.47}As$ quantum cylinder, as functions of the wave vector (in units of E_0).

The effective-mass parameters used in the calculation are listed in table 1. We calculated the hole energy levels ($L = 0$) of the $In_{0.53}Ga_{0.47}As$ quantum cylinder as functions of the spin–orbital splitting parameter λ for $k_z = 0$, and of the wave vector k_z for $\lambda = 13$, as shown in figures 1 and 2, respectively. In figures 1 and 2 the unit of the energy is taken as

$$E_0 = \frac{\gamma_1}{2m_0}\left(\frac{\eta}{R}\right)^2 \tag{15}$$

where R is the radius of the cylinder. Therefore the energies of the quantum states in the quantum cylinder are inversely proportional to the square of the radius. From figure 1 we see that as λ becomes large, the ground state and low-lying excited states approach those in the strong-SOC limit; note that when λ is small the energy levels are more complicated. For a specific material, λ ($=\Delta/3E_0$) is not a constant: it depends on the radius R. For the $In_{0.53}Ga_{0.47}As$, with $\Delta = 0.362$ eV, λ equals 2.84 and 13.1 for $R = 35$ and 75 Å, respectively. From figure 2 we see that the one-dimensional subbands are not parabolic as in the electronic case, due to the interaction between the heavy and light holes. Some subbands have negative effective mass near $k_z = 0$.

The PL spectra calculated using equations (12)–(14), including the azimuthal angular momentum $L = 0, 1, 2$, for an $In_{0.53}Ga_{0.47}As$ wire of radius 75 Å at the temperatures 2 and 300 K are shown in figures 3(a) and 3(b), respectively. In all calculations of the PL spectra in this paper, the Lorentz linewidth Γ in equation (12) is taken as 50 meV. From figure 3 we see that the PL spectra have apparent polarization anisotropy, and that the PL intensities for polarization parallel to the wire are larger than those for polarization perpendicular to the wire. When the temperature increases, the PL peaks shift in the high-energy direction, and the degree of polarization (equation (11)) decreases. Figure 4 shows the degrees of polarization P as functions of temperature for $In_{0.53}Ga_{0.47}As$ wires of radii 35 and 75 Å. From figure 4 we see that, for thin wire ($R = 35$ Å), P ($=0.8$) basically does not vary with the temperature, while for thicker wires, P decreases with the temperature. The theoretical results in figure 3(a) are very similar to the experimental results for the $In_{0.53}Ga_{0.47}As$ quantum wire with a nearly square cross section (see figure 2 in reference [7] for $L_x = 16$ nm). Therefore the valence band structure is the main cause of the linear polarization of the luminescence in quantum wires.

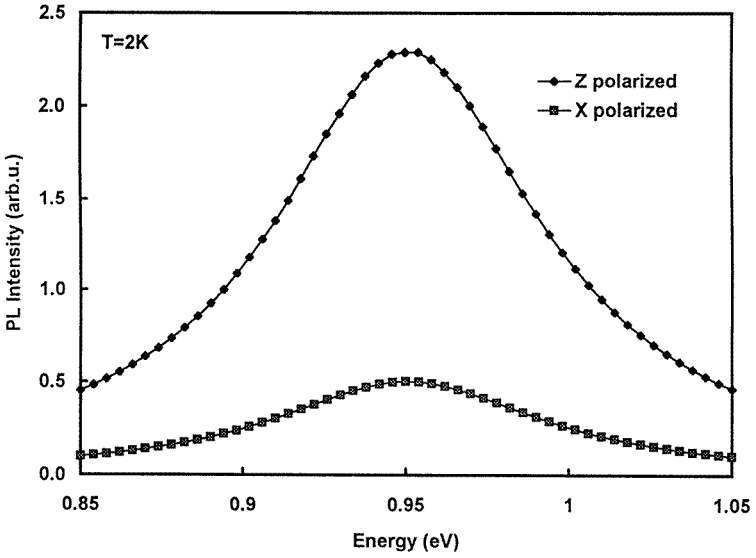

(a)

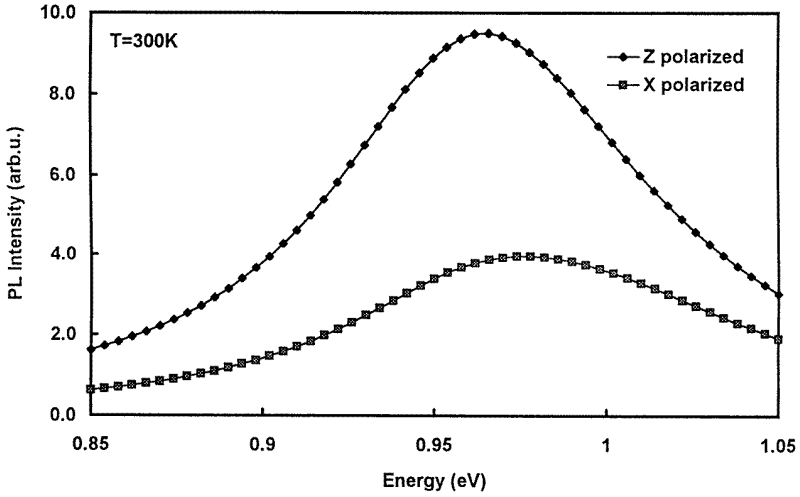

(b)

Figure 3. PL polarization spectra for an $In_{0.53}Ga_{0.47}As$ quantum cylinder of radius 75 Å at (a) 2 K, and (b) 300 K.

The linear character of the polarization can be further explained by the wave function of the ground state in the quantum wire. From the calculation we found that the contribution of the hole's lowest ground states to the luminescence is mainly for polarization parallel to the wire. In the case of thin wire and low temperature, the electron transfers mainly to the hole ground states, resulting in a large degree of polarization. For thicker wire and high temperature, the electron has a larger possibility of transferring to excited states; this contributes to the luminescence of perpendicular polarization, thus reducing the degree of polarization.

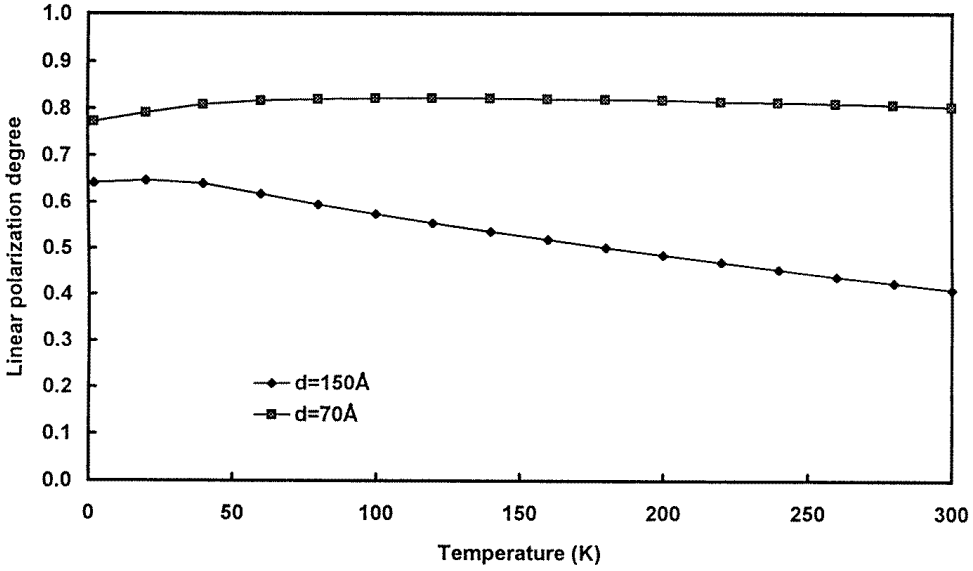

Figure 4. Degrees of linear polarization as functions of temperature for $In_{0.53}Ga_{0.47}As$ quantum cylinders of radii 35 and 75 Å.

4. Experimental results for porous silicon

The two samples used in this experiment were fabricated from n-type silicon (100) wafers with resistivities of 5–8 Ω cm using electrochemical anodization. The etching conditions were as follows. For sample A (whn002), the anodic etching was carried out in a solution which was a mixture of HF (50 wt% in water) and ethanol, 1:1 by volume, at a constant current density of 15 mA cm^{-2} for 30 min. For sample B (whn004), the anodization was carried out in a 2:1 volume mixture of HF (50 wt% in water) and ethanol at a current density of 20 mA cm^{-2} for 60 min. The distance between the Si and Pt (the cathode) was 4 cm. After etching, the samples were dried in air. At room temperature, the PL intensity was bright enough to see with the naked eye when the sample was exposed to UV radiation or excited by an argon laser.

In the variable-temperature PL set-up, a He–Cd laser (the 325 nm laser line) was used as an excitation source, and the sample temperature was varied from 10 K to room temperature in an OXFORD cryostat system. The PL signal was collected through a polarizer via a lens entrance slit of a double monochromator (ORIEL Corporation) with a focal length of 25 cm, and was detected by a Peltier-cooled PMT (Hamamatsu R656) whose response curve is flat over the range 300 nm to 900 nm. The electronic signal from the PMT was amplified by an EG&G Model 5182 current preamplifier, and processed by a computer.

We defined the x-, y-, and z-axes as shown in the inset of figure 5: the surface of the sample is an x–y plane, and the (100) direction is that of the z-axis. For this experimental geometry, the polarization direction of the incident beam was not aligned in any particular direction, and the incident beam was parallel to the z-axis. The direction of PL signal collection was along the y-axis. Therefore, the electric field vectors of the PL signal were either in the z- or x-axis direction (the PZ or PX mode, respectively) when the direction of the polarizer was parallel to the z- or x-axis, respectively. That means that $I_{\parallel}$ in equation (11)

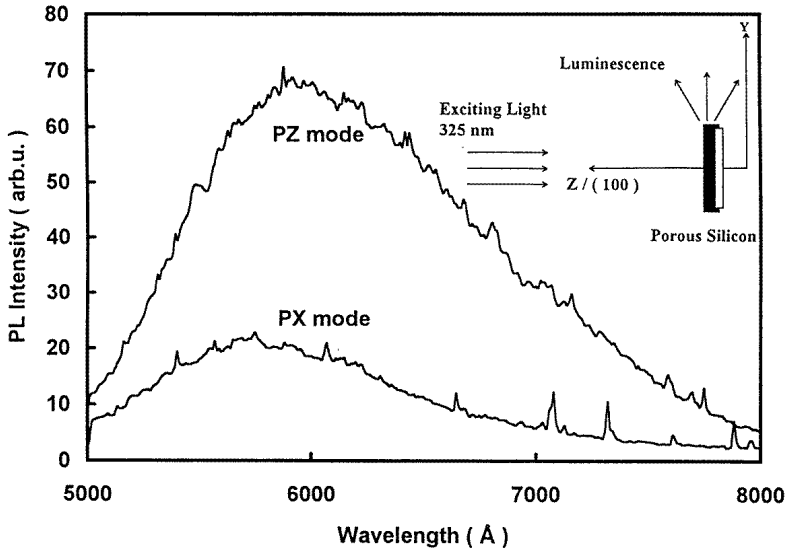

Figure 5. PL polarization spectra of porous Si, at 30 K; the polarization modes were PZ and PX. The spectra showed that the PL intensity of the PZ mode was significantly greater than that of the PX mode. The inset shows how the x-, y-, and z-axes are defined: the z-axis is parallel to the (100) crystal direction of porous silicon, the x-axis is parallel to the PL signal collection direction, and the x–y plane is parallel to the surface of the porous silicon.

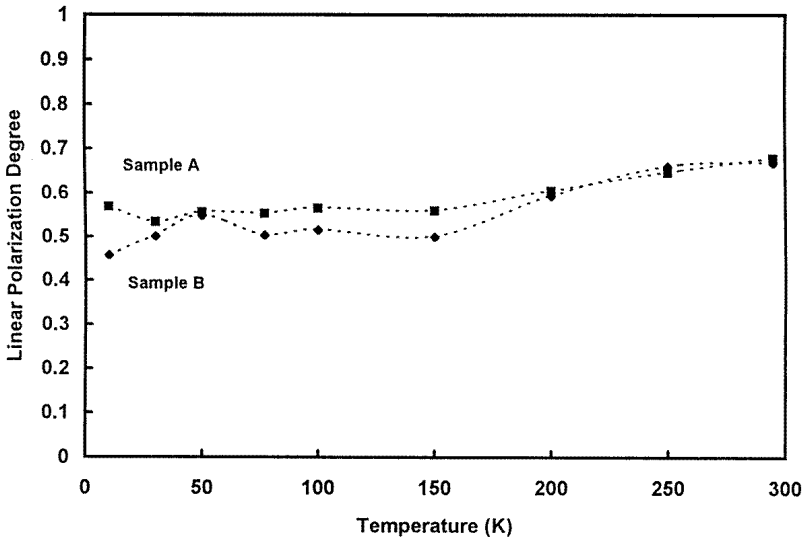

Figure 6. Linear degrees of polarization of porous silicon as functions of the temperature.

is the intensity of the photoluminescence from the PZ mode, and that $I_{\perp}$ in equation (11) is that from the PX mode.

For these two samples, the temperature-dependent PL measurements were taken at the same power excitation, 80 μW. Moreover, the excitation power density, 8 mW cm^{-2},

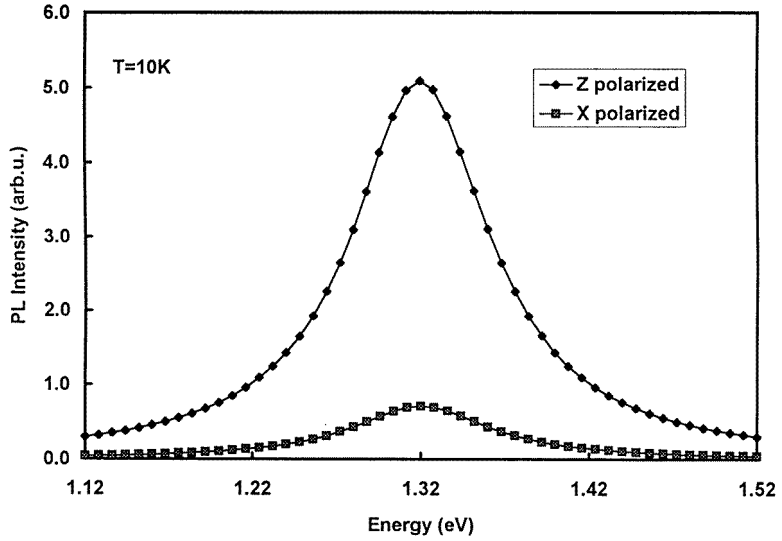

(a)

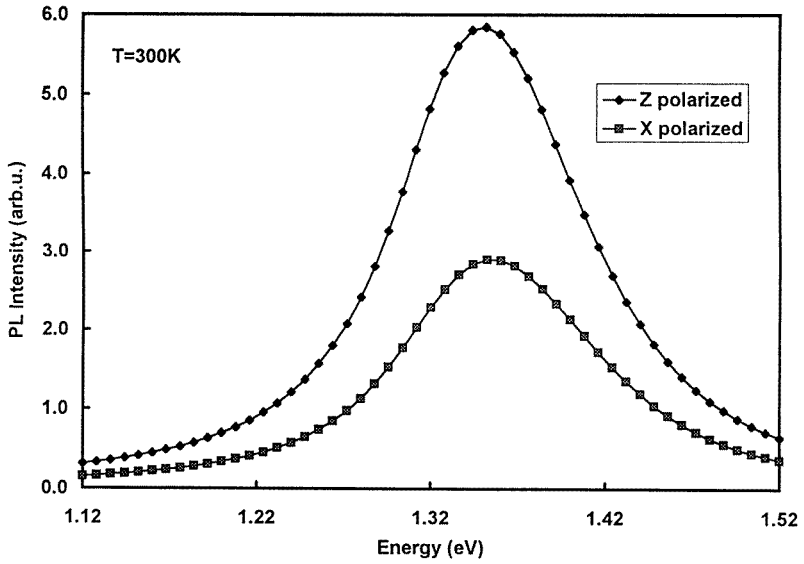

(b)

Figure 7. PL polarization spectra for a porous silicon sample of radius 75 Å at (a) 10 K, and (b) 300 K.

was kept sufficiently low that irradiation-induced degradation was avoided. During each measurement, the samples were maintained at constant temperature. Figure 5 shows typical PL spectra at 30 K. It shows that the intensity of the PZ mode is significantly greater than that of the PX mode. The degrees of linear polarization of sample A and sample B are shown in figure 6 as functions of temperature. From figure 6 we can see that the average degree of linear polarization, P, can be as high as 50% in the two samples.

5. Discussion of the porous silicon results

As reported in references [13–15], and from our experimental results, the photoluminescence of porous Si also shows anisotropic linear polarization. This proves that the luminescence in porous Si is connected with the hole states formed by the quantum confinement effect, while excluding some luminescence centres—for example, siloxene, whose polarization has no linear character. Although the porous silicon structure is generally considered to have wires in a random orientation, it is possible that these wires have a preferred orientation. This is because in anodization there is a driving direction for the anodizing current, so the wires fabricated by anodization can be directional [18]. As for the electronic states, it is commonly recognized that the quantum confinement effect is too small to explain the large luminescence efficiency of porous Si. Here we make a phenomenological assumption about the electronic states in porous Si: the electronic state is localized in the surface layer potential well, and has Γ character [19, 20]. The electron can transfer directly to the hole states, but, due to its localization, the ordinary selection rule $\Delta n = 0$ will not be followed.

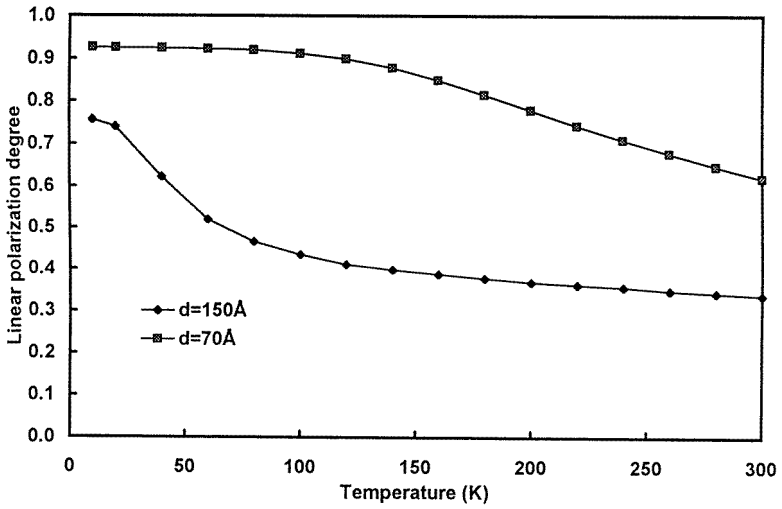

Figure 8. Degrees of polarization as functions of the temperature for porous silicon samples of radii 35 and 75 Å.

Because the porous Si in our experiment is n-type, we assume that the distribution function of the surface electronic states in equation (12) is also a Maxwell distribution, like equation (13). Similarly we calculated the PL spectra of the porous Si for different wire radii and temperatures. PL spectra of porous Si wire of radius 75 Å at temperatures of 10 and 300 K are shown in figures 7(a) and 7(b), respectively. From figure 7 we see that the PL spectra of the porous Si also show anisotropic linear polarization, and that the degree of polarization decreases as the temperature increases. The degrees of polarization as functions of temperature for wires of radii 35 and 75 Å are shown in figure 8, from which we see that the degree of polarization decreases with rising temperature faster than those for $In_{0.53}Ga_{0.47}As$ quantum wires. Even for the thin wire ($R = 35$ Å), the degree of polarization exhibits an obvious drop. This is because of the properties of the surface electronic states, which transfer not only to the hole ground states, but also have a definite probability of transferring to the excited states with perpendicular polarization.

Our theoretical results are qualitatively in agreement with our experimental results (figures 5 and 6) and other experiments; moreover the degrees of polarization are between that of 35 Å silicon wires and that of 70 Å silicon wires. In fact, porous Si is a mixture of silicon clusters and wires, while the luminescence of the silicon cluster does not have linear polarization in a specific direction. Furthermore, silicon wires in porous silicon are not necessarily spatially oriented in the same direction, as in the case of InGaAs quantum wires fabricated by electron-beam lithography. Besides this, the radii of the silicon wires are not uniform. All of these factors together reduce the degree of polarization of the luminescence in porous Si. But, from the fact that the luminescence of the porous Si has anisotropic linear polarization, it is concluded that the luminescence of porous Si is connected with internal electronic states in quantum confinement, into which the optical transition occurs. In addition, from our experiment, the degree of polarization is almost independent of the temperature. This is in conflict with our theoretical results. We attribute this difference to the fact that in our theoretical consideration we assume that there is a significant contribution from the excited hole states. However, the excitation power in our experiment was too weak to induce a significant contribution from these states.

6. Summary

In this paper we have studied the linear character of the polarization of the luminescence in porous Si experimentally, and applied a quantum cylindrical model in the framework of the effective-mass theory to explain the linear character of the polarization of the luminescence in quantum wires. From the experimental and theoretical results, it is concluded that there is stronger linear polarization parallel to the wire direction than perpendicular to the wire, and that it is connected with the valence band structure in quantum confinement in two directions. Theoretical PL spectra for parallel and perpendicular polarization directions, and the degrees of polarization as functions of the radius of the wire, the temperature, and the exciting intensity, are obtained for $In_{0.53}Ga_{0.47}As$ quantum wires and porous silicon. From the theory, we found that the degree of polarization decreases with increasing temperature and radius, and that this effect is more apparent for porous Si. However, the degree of polarization was independent of the temperature, because few of the excited hole states contribute to the luminescence in our experiment. Nevertheless, the theoretical results agree well with the experimental results for the InGaAs quantum wires, and agree qualitatively with those for porous silicon.

Acknowledgment

This work was supported by a Croucher Foundation Research Grant.

References

[1] Arakawa Y and Sakaki H 1982 *Appl. Phys. Lett.* **40** 939
[2] Schmit-Rink S, Miller D A B and Chemla D S 1987 *Phys. Rev.* B **25** 8113
[3] Reed M A, Randall N, Aggarwal R J, Matye R J, Moore T M and Westel A E 1988 *Phys. Rev. Lett.* **60** 535
[4] Kash K, Scherer A, Worlock J M, Craighead H G and Tamargo M C 1986 *Appl. Phys. Lett.* **49** 1043
[5] Gershoni D, Temkin H, Dolan G, Dunsmuir J, Chu S N G and Panish M B 1988 *Appl. Phys. Lett.* **53** 995
[6] Kohl M, Heitmann D, Grambow D and Ploog K 1989 *Phys. Rev. Lett.* **63** 2124
[7] Ils P, Greus C, Forchel A, Kulakovskii V D, Gippius N A and Tikhodeev S G 1995 *Phys. Rev.* B **51** 4272
[8] Cibert J, Petroff P M, Dolan G J, Pearton S J, Gossard A C and English J H 1986 *Appl. Phys. Lett.* **49** 1275
[9] Kapon E, Hwang D M and Bhatt R 1989 *Phys. Rev. Lett.* **63** 430

[10] Notzel R, Ledentsov N N, Daweritz L, Hohenstein M and Ploog K 1991 *Phys. Rev. Lett.* **67** 3812
[11] Gershoni D, Weiner J S, Chu S N G, Baraff G A, Vanderberg J M, Pfeiffer L N, West K, Logan R A and Tanbun-Ek T 1990 *Phys. Rev. Lett.* **65** 1631
[12] Canham L T 1990 *Appl. Phys. Lett.* **57** 1046
[13] Kovalev D, Ben Chorin M, Diener J, Koch F, Efros Al L, Rosen M, Gippius N A and Tikhodeev S G 1995 *Appl. Phys. Lett.* **67** 1585
[14] Gaponenko S V, Kononenko V K, Petrov E P, Gemanenko I N, Stupak A P and Xie Y H 1995 *Appl. Phys. Lett.* **67** 3019
[15] Koyama H and Koshida N 1995 *Phys. Rev.* B **52** 2649
[16] Xia J B 1996 *J. Lumin.* **70** 120
[17] Luttinger J M 1956 *Phys. Rev.* **102** 1030
[18] Schuppler S, Friedman S L, Marcus M A, Adler D L, Xie Y H, Ross F M, Chabal Y J, Harris T D, Brus L E, Brown W L, Chaban E E, Szajowski P F, Christman S B and Citrin P H 1995 *Phys. Rev.* B **52** 4910
[19] Xia J B and Cheah K W 1994 *Appl. Phys.* A **59** 227
[20] Cheah K W, Ho L C, Xia J B, Li J, Zheng W H, Zhuang W R and Wang Q M 1995 *Appl. Phys.* A **60** 601